A Compact Meander-Line UHF RFID Tag Antenna Loaded With Elements Found in Right/Left-Handed Coplanar Waveguide Structures

Benjamin D. Braaten, *Member, IEEE*, Michael Reich, *Member, IEEE*, and Jacob Glower, *Member, IEEE*

***Abstract*—A new planar meander-line antenna for passive UHF radio frequency identification (RFID) tags is presented. Specifically, a meander-line antenna is loaded periodically with coplanar waveguide (CPW) *LC* elements traditionally found in right/left-handed waveguide structures. It is shown that by using the antenna presented in this letter in a prototype passive UHF RFID tag, effective read ranges up to 4.87 m can be achieved. Many different dielectric substrates and CPW-*LC* load dimensions are investigated to illustrate how the input impedance, gain, and overall dimensions of the antenna are affected by these structural differences. It is shown that the overall dimension of the meander-line antenna can be reduced by slightly more than 18% with the introduction of the CPW-*LC* elements to the design. Several of the simulation results are validated by comparison with measurements.**

***Index Terms*—Coplanar waveguide (CPW) and passive tag, dipole, meander-line, metamaterial, radio frequency identification (RFID).**

I. Introduction

A NEW AND promising field of research that investigates the use of metamaterials to reduce the overall size of printed antennas is resulting in much physically smaller antennas. These smaller metamaterial-based antennas have the radiation properties and impedance values of much larger resonant printed antennas found in communications [1]–[5] and radio frequency identification (RFID) systems [6], [7]. Some of the drawbacks of using metamaterial-based antennas are the complicated ground planes, vias, lumped elements, and materials required to reduce the overall size of the antenna (with the exception of [3]). In many cases, these complicated structures are not suitable for passive RFID applications. This is because many of the antennas on passive RFID tags are printed on a single conducting plane with a single dielectric substrate [8]–[10]. Therefore, using the techniques in [1]–[7] to reduce the size of a RFID antenna may render the RFID tag too complex and costly to deploy in passive RFID applications.

Manuscript received September 16, 2009. First published October 30, 2009; current version published November 10, 2009. This work was supported in part by the Defense Microelectronics Activity under Agreement H94003-08-2-0804.

B. D. Braaten and J. Glower are with the Department of Electrical and Computer Engineering, North Dakota State University, Fargo, ND 58102 USA (e-mail: benbraaten@ieee.org; Jacob.Glower@ndsu.edu).

M. Reich is with the Center for Nanoscale Science and Engineering, North Dakota State University, Fargo, ND 58102 USA (e-mail: mike.reich@ndsu.edu).

Color versions of one or more of the figures in this letter are available online at http://ieeexplore.ieee.org.

Digital Object Identifier 10.1109/LAWP.2009.2034990

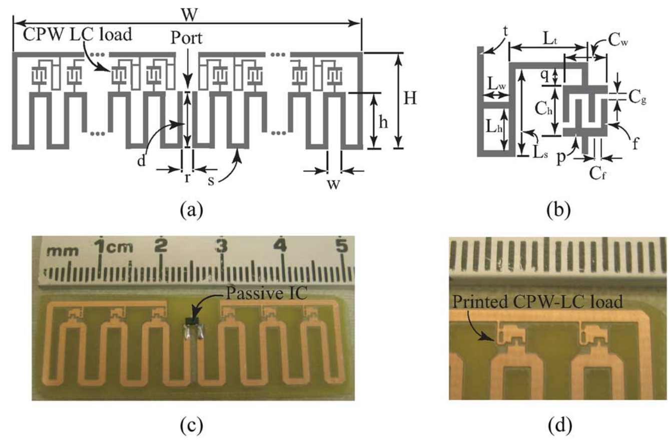

Fig. 1. (a) Meander-line antenna with CPW-*LC* loads. (b) Dimensions of the CPW-*LC* loads. (c) Printed *LC*-loaded meander-line antenna on the prototype passive RFID tag (t $= 0.225$ mm, $L_w = 0.28$ mm, $L_h = 0.92$ mm, $L_s = 1.42$ mm, $L_t = 0.72$ mm, q $= 0$ mm, $C_h = 2.17$ mm, p $= 0.64$ mm, $C_f = 0.29$ mm, $C_w = 1.49$ mm, $C_g = 0.3$ mm, f = .31 mm, s = 1.06 mm, w = 2.22 mm, W = 47.13 mm, 11.03 mm, H = 14.81 mm, r = 1.04 mm, and d $= 10.59$ mm. (d) CPW-*LC* loads along the meander-line antenna.

In this letter, interdigitated capacitors (*C*) and shunt inductors (*L*) are used to reduce the overall size of a meander-line antenna on a passive UHF RFID tag. In particular, this is done by periodically loading the meander-line antenna in Fig. 1(a) with the series coplanar waveguide (CPW) interdigitated capacitors and inductors found in the right/left-handed structures recently presented in [11]. The dimensions of the CPW-*LC* loads are shown in Fig. 1(b). The antenna presented in this letter is a new approach to designing meander-line antennas and has resulted in the following very useful features: 1) the RFID antenna can be printed on a single dielectric substrate (i.e., thin adhesives), which makes the antenna easy to manufacture; 2) a ground plane is not required for efficient radiation of the RFID antenna; 3) the RFID antenna has a gain comparable to other planar meander-line antennas at or around the same center frequency [12]–[14]; 4) discrete components are not required to introduce the series capacitance and inductance in the antenna, thus keeping the cost of the tag much lower; and finally 5) the RFID antenna has a pattern similar to a small dipole.

II. Performance of the Meander-Line Antenna Loaded With Right/Left-Handed CPW Structures

It is often desirable to describe an antenna with an equivalent circuit. In this case, each pole of the meander-line antenna in Fig. 1(a) has an equivalent capacitance C_{eq} between the longer parallel vertical traces and an equivalent inductance

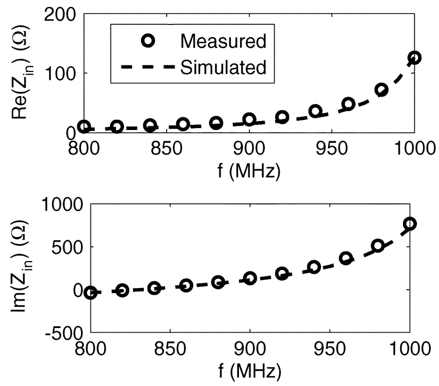

Fig. 2. Input impedance results for the printed antenna on the prototype RFID tag.

L_{eq} as a result of the horizontal traces [15]. This results in a parallel connected $L_{eq}C_{eq}$ equivalent circuit for each meander-line section. By periodically loading the meander-line sections with the CPW-*LC* circuit, the equivalent circuit of each meander-line section is changed to C_{eq} connected in parallel with two series connected inductances of $L_{eq}/2$ with one end of the series CPW-*LC* circuit connected to a node between the two $L_{eq}/2$ inductance values. This added CPW-*LC* impedance is used to add inductance (or capacitance if desired) to the input impedance of an electrically small meander-line antenna. The result is a smaller meander-line antenna. This inductance is important because electrically small antennas can have a significant input capacitance [15].

A. Experimental Results and Validation

To determine if the design in Fig. 1(a) performed well, a prototype tag was manufactured. Momentum [16] was used to design the printed antenna on a FR-4 ($\varepsilon = 3.7$ measured and $\tan\delta = .0011$ measured) substrate with a thickness of 1.36 mm. The passive IC on the prototype RFID tag chosen was the Higgs-2 by Alien Technologies [17]. At 920 MHz, the Higgs-2 IC[1] has an input impedance of approximately $Z_{\rm IC} = 13.6 -$ j142.8 Ω [17]. This requires the printed antenna design on the prototype tag to have an input impedance close to the conjugate of $Z_{\rm IC}$ at 920 MHz. These requirements resulted in the printed antenna design shown in Fig. 1(c) with a closer image of the CPW-*LC* loads shown in Fig. 1(d). Notice that the CPW-*LC* loads shown in Fig. 1(b) are slightly different than the manufactured loads in Fig. 1(d). This is due to the limitation of the milling machine used to manufacture the prototype tag. Because a 0.2032-mm (8-mil) cut is the smallest size available for manufacturing the tag, the antenna had to be designed with fewer capacitive fingers and an inductor that would be easy to mill from the side of the capacitor. To measure the input impedance, the printed antenna was cut symmetrically down the middle, placed vertically above a ground plane (1.2 m × 2.7 m), and fed with an SMA connector through the ground plane. The input impedance was then measured using a calibrated network analyzer. The measured and simulated input impedance results are shown to agree very well in Fig. 2.

[1]The sensitivity during a read is −14 dBm, and the sensitivity during programming is −10 dBm. Also, the equivalent input impedance is a 1.5-KΩ resistor connected in parallel with a 1.2-pF capacitor [17].

TABLE I
MEASURED READ RANGE OF THE PROTOTYPE TAG ON VARIOUS MATERIALS

Item	Read range (m)	Comments
Styrofoam	4.87	3 cm thick
Paper	3.35	single ream
Plastic container	3.50	empty
Carpet	4.26	foam backed
Clothing	4.26	10 cm thick
Sheetrock	3.35	1.58 cm thick

B. Measured Read Range of the Prototype Tag on Various Items

The next step in the validation process was to determine how well the prototype tag in Fig. 1(c) performed on various materials. This was done by placing the prototype tag on the different materials listed in the first column of Table I. Then, an Alien Technologies ALR-9900 RFID reader [17] (with a maximum output power of 1 W) connected to a CP antenna with a gain of 6 dBi and the material with the tag attached on the surface were placed in an anechoic chamber. Next, the max read range of the tag on the different materials was determined using the method described in [9]. The results from these measurements are shown in the second column of Table I. The max read range of the tag was 4.87 m. This max read range is comparable to many commercially available tags.[2] When compared to the dimensions of certain commercial tags, the prototype tag presented in this letter is 47%–70% smaller (i.e., the prototype tag has 47%–70% less surface area than several of the tested commercial tags). This reduced size is achieved by using a thicker substrate and the CPW-*LC* loads in Fig. 1(d).

The accurate results in Fig. 2 and the good read range values in Table I indicate that there is a good conjugate match between the Higgs-2 IC and the antenna. This in turn demonstrates that Momentum is a good and accurate tool for modeling the antenna in Fig. 1(c). Therefore, because of the large number of designs in the next section, Momentum will be used exclusively to calculate the input impedance and gain of the various antennas. In particular, Momentum will be used to calculate the input impedance and gain of the antenna in Fig. 1(c) on various values of permittivity, substrate thicknesses, and CPW-*LC* dimensions (i.e., C_g and L_w values). This will show how the impedance and gain of the antenna changes for different substrate properties and CPW-*LC* dimensions. These results will be very useful for a designer using this type of RFID antenna because the following sections will demonstrate the behavior of the antenna.

C. Results for Various Substrate Properties and CPW-LC Loads

Initially, the thickness d of the substrate was changed and ε was fixed at 4.25. This illustrated how the input impedance and gain changed as the thickness was increased. The results from these simulations are shown in Figs. 3 and 4. The results in Fig. 3 show that the input resistance can increase dramatically for larger values of d and that the antenna becomes more inductive for larger values of d. The results in Fig. 4 show a max

[2]The max read range values for several commercial tags manufactured by Alien Technology [17] and Invengo [18] were also determined in the anechoic chamber with various Alien Technology RFID readers.

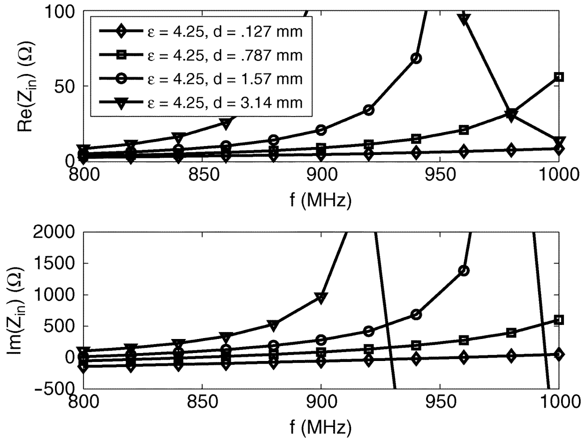

Fig. 3. Input impedance for various values of d.

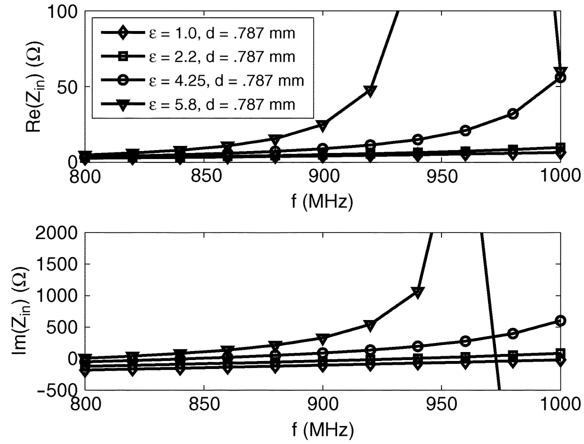

Fig. 5. Input impedance for various values of ε.

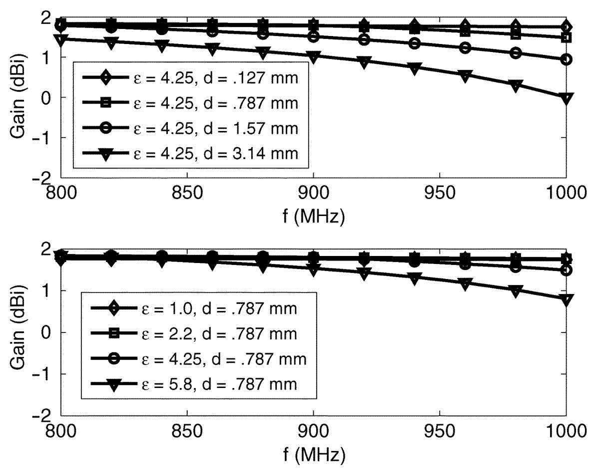

Fig. 4. Gain for various values of d and ε.

TABLE II
COMPUTED OVERALL SIZE RELATION OF THE PROTOTYPE TAG FOR VARIOUS SUBSTRATE PROPERTIES AND CPW-*LC* LOADS

line	d (mm)	ε	A (mm^2)	CPW-LC loads
1	1.36	3.6	697	yes
2	1.36	3.6	849	no
3	1.0	3.6	743	yes
4	.5	3.6	829	yes
5	0	1.0	1093	yes

gain of 1.84 dBi and that the gain can be significantly reduced for larger values of d.

Next, the permittivity ε of the substrate was changed and d was fixed at 0.787 mm. Again, this illustrated the behavior of the input impedance and gain as the values of ε were changed. The results from these simulations are shown in Figs. 4 and 5. The results in Fig. 4 show a max gain of 1.84 dBi and that the gain reduces for larger values of ε. The results in Fig. 5 show how much the input resistance can increase for larger values of ε and how the antenna becomes more inductive for larger values of ε. For the dimensions in Fig. 1(c), the antenna performs well for smaller values of ε and d. This indicates that the CPW-*LC* loaded meander-line antenna presented in this letter is very suitable for printing on thin adhesive substrates.

Next, the substrate thickness and CPW-*LC* loads were altered and the overall surface area A of the antenna on the tag was computed. This was done to show how the substrate values and CPW-*LC* loads individually altered the size of the antenna on the prototype tag. The results from these computations are shown in Table II. The entries in the first line are for the antenna on the prototype tag in Fig. 1(c). The second line shows the area of the prototype antenna in Fig. 1(c) with the CPW-*LC* loads along the folded ends removed. When the input impedance and gain matched the values of the prototype antenna in Fig. 1(c), the surface area of the antenna was computed. This procedure resulted in an antenna with an overall area of 849 mm^2, which is 21.8% larger than the antenna on the prototype tag. This shows the actual size reduction due solely to the CPW-*LC* loads along the meander-line antenna. The third line shows the area of the prototype antenna in Fig. 1(c) with the CPW-*LC* in place along the folded ends and the substrate thickness reduced to 1.0 mm. Again, when the input impedance and gain matched the values of the prototype antenna in Fig. 1(c), the surface area of the antenna was computed. This procedure resulted in an antenna with an overall area of 743 mm^2, which is 6.59% larger than the antenna on the prototype tag. This shows the actual size reduction due solely to the substrate thickness. Also, lines 4 and 5 show the area of the prototype antenna with a smaller substrate (0.5 mm) and in free space. The prototype antenna is 56.8% larger in free space.

Next, the structure of the CPW-*LC* loads were modified, and the input impedance was determined for various values of loop inductance L_w with ε and d set at 4.25 and 0.787 mm, respectively. The simulated input impedance is shown in Fig. 6. It is shown that the input resistance varies by only a few Ohms over the range of L_w, but the input reactance varies by as much as 80 Ω over the range of L_w. Finally, the input impedance was determined for various values of gap-capacitance C_g with ε and d set at 4.25 and .787 mm, respectively. The simulated input impedance is shown in Fig. 7. It is shown that the input resistance varies by approximately 7 Ω over the range of C_g, but the input reactance varies by as much as 145 Ω over the range of C_g. This shows that the capacitor portion of the CPW-*LC* load can be used to match the entire antenna impedance with the tag.

III. DISCUSSION

Many important comments can be made about the results in Figs. 1 and 3–7 and Tables I and II.

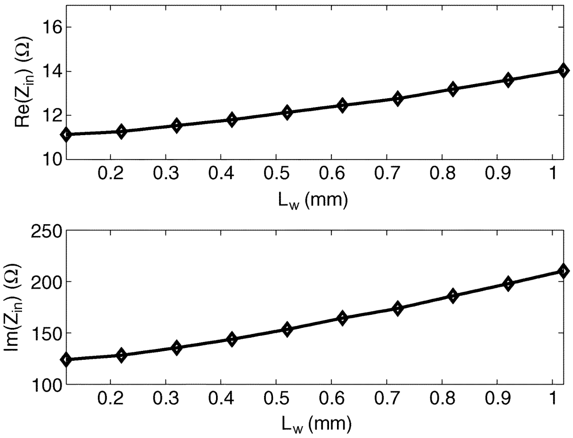

Fig. 6. Input impedance for various values of L_w.

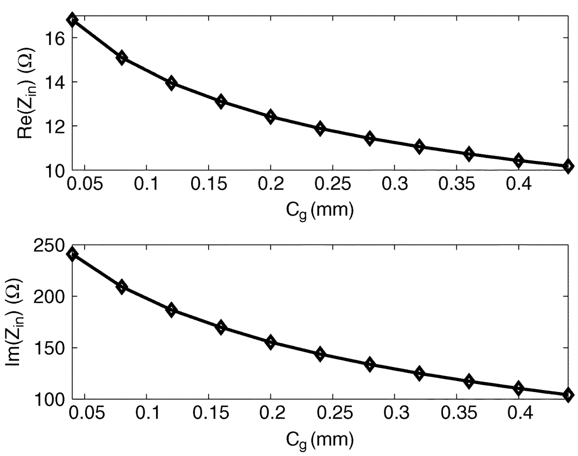

Fig. 7. Input impedance for various values of C_g.

1) Combining the dimensions in Fig. 1(c) with the results in Table I shows that the antenna presented in this letter can be used in a compact tag design that is very useful on many common items found in manufacturing.
2) The results in Table II show that the size of the meander-line antenna can be reduced by 18% by simply introducing the CPW-*LC* loads.
3) From the results in Figs. 3–5, it can be concluded that the CPW-*LC* loaded meander-line antenna presented in this letter is suited for printing on very thin substrates.
4) The results in Figs. 6 and 7 show that both the loop inductance and gap-capacitance can be used effectively to match the input impedance of the antenna with the impedance of the tag ($Z_{\mathrm{IC}} = 13.6 - \mathrm{j}142.8\ \Omega$).

IV. Conclusion

A new compact CPW-*LC* loaded meander-line antenna has been presented. A prototype tag was printed on FR-4 material, and several of the simulated input impedance values were validated by comparison with measurements. It was shown that the prototype tag had effective read range values on various common manufactured materials while having overall dimensions that were 47%–70% less than commercially available tags. Finally, many different dielectric substrates and CPW-*LC* load dimensions were investigated to illustrate how the input impedance, gain, and overall size of the antenna were affected by these structural differences.

Acknowledgment

The authors would like to thank A. Reinholz at the Center for Nanoscale Science and Engineering (CNSE), North Dakota State University, Fargo, for supporting various aspects of this project. The United States Government is authorized to reproduce and distribute reprints for government purposes, notwithstanding any copyright notation thereon.

References

[1] R. W. Ziolkowski and C.-C. Lin, "Metamaterial-inspired magnetic-based UHF and VHF antennas," in *Proc. IEEE Antennas Propag. Soc. Int. Symp. Dig.*, San Diego, CA, Jul. 5–11, 2008, pp. 1–4.
[2] C.-J. Lee, K. M. K. H. Leong, and T. Itoh, "Composite right/left-handed transmission line based compact resonant antennas for RF module integration," *IEEE Trans. Antennas Propag.*, vol. 54, no. 8, pp. 2283–2291, Aug. 2006.
[3] H. Iizuka and P. S. Hall, "Left-handed dipole antennas and their implementations," *IEEE Trans. Antennas Propag.*, vol. 55, no. 5, pp. 1246–1253, May 2007.
[4] M. A. Y. Abdalla, K. Phang, and G. V. Eleftheriades, "A planar electronically steerable patch array using tunable PRI/NRI phase shifters," *IEEE Trans. Microw. Theory Tech.*, vol. 57, no. 3, pp. 531–541, Mar. 2009.
[5] F. J. Herraz-Martinez, P. S. Hall, Q. Liu, and D. Segovia-Vargas, "Tunable left-handed monopole and loop antennas," in *Proc. IEEE Antennas Propag. Soc. Int. Symp. Dig.*, Charleston, SC, Jun. 1–5, 2009, pp. 1–4.
[6] J. Dacuna and R. Pous, "Miniaturized UHF tags based on metamaterials geometries," July 2007, Building Radio Frequency Identification for the Global Environment [Online]. Available: www.bridge-project.eu
[7] M. Stupf, R. Mittra, J. Yeo, and J. R. Mosig, "Some novel design for RFID antennas and their performance enhancement with metamaterials," *Microw. Opt. Technol. Lett.*, vol. 49, no. 4, pp. 858–867, Feb. 2007.
[8] G. Marrocco, "Gain-optimized self-resonant meander line antennas for RFID applications," *IEEE Antennas Wireless Propag. Lett.*, vol. 2, pp. 302–305, 2003.
[9] K. V. S. Rao, P. V. Nikitin, and S. F. Lam, "Antenna design for UHF RFID tags: A review and a practical application," *IEEE Trans. Antennas Propag.*, vol. 53, no. 12, pp. 3870–3876, Dec. 2005.
[10] C. T. Rodenbeck, "Planar miniature RFID antennas suitable for integration with batteries," *IEEE Trans. Antennas Propag.*, vol. 54, no. 12, pp. 3700–3706, Dec. 2006.
[11] S.-G. Mao, Y.-Z. Chueh, and M.-S. Wu, "Asymmetric dual-passband coplanar waveguide filters using periodic composite right/left-handed and quarter-wavelength stubs," *IEEE Microw. Wireless Compon. Lett.*, vol. 17, no. 6, pp. 418–420, Jun. 2007.
[12] H.-K. Ryu and J.-M. Woo, "Small-sized square loop antenna using meander line for RFID tag applications," in *Proc. IEEE Antennas Propag. Soc. Int. Symp. Dig.*, Jun. 9–15, 2007, pp. 2463–2466.
[13] T. Bjorninen, M. Nikkari, L. Ukkonen, F. Yang, A. Elsherbeni, L. Sydanheimo, and M. Kivikoski, "Design and RFID signal analysis of a meander line UHF RFID tag antenna," in *Proc. IEEE Antennas Propag. Soc. Int. Symp. Dig.*, San Diego, CA, Jul. 5–11, 2008, pp. 1–4.
[14] Y. Amin, S. Batao, J. Hallstedt, S. Prokkola, H. Tenhunen, and L.-R. Zheng, "Design and characterization of efficient flexible UHF RFID tag antennas," in *3rd Eur. Conf. Antennas Propag.*, Mar. 23–27, 2009, pp. 2784–2786.
[15] R. Bancroft, *Microstrip and Printed Antenna Design*. Raleigh, NC: Scitech, 2006, pp. 194–195.
[16] Advanced Design System–ADS 2009. Agilent Technologies.
[17] Alien Technologies. [Online]. Available: www.alientechnology.com
[18] Invengo Information Technology Co., Ltd. [Online]. Available: www.invengo.com